Development of High Erosivity Well Scale Cleaning Tools

K.M. Kalumuck, G.L. Chahine,
G.S. Frederick and P.D. Aley

July 1999

This work was conducted under Contract No. DE-FG07-981D13684 for the U.S. Department of Energy, Idaho Operations Office, Idaho Falls, ID

DISCLAIMER

1. INTRODUCTION

1.1 Overview

Build up of scale deposits on the walls of geothermal wells can occur rapidly due to the high dissolved solids content of geothermal fluids, e.g., up to 250,000 ppm in the Salton Sea geothermal field [1]. Scale formation is a significant problem for both the well and for surface heat transfer equipment. Geothermal brines contain a wide variety of dissolved salts including carbonates, silicates, sulfates, and metal sulfides. Currently this is dealt with either by the use of chemical additives to inhibit scale formation or the periodic removal of scale through the use of a workover rig drill bit, high pressure water jets, or acids. However, such procedures are costly. Chemical inhibitors do not currently exist for silica scales [1, 2], and their use raises environmental concerns.

One technology recently proposedfor scale removal is the use of an ultrasonic device. The recent Advanced Geothermal Drilling Systems Workshop [1] recommended further exploration of this concept. Cleaning occurs due to the excitation of the growth and collapse of cavitation bubbles by the high frequency acoustic waves. In the present effort we apply cavitation in a more direct manner by the use of acoustically enhanced cavitating water jets which can be made to be much more efficient and aggressive than ultrasonic devices.

Cavitating and self-resonating jet technologies have been proven to enhance the erosive power of liquid jets in a number of cutting, cleaning, and drilling applications. Removal of harder scales, such as calcium carbonate, barium sulphate, strontium sulphate, and silicates is a particularly good area of potential application for this technology as the relative improvement in erosivity of cavitating and interrupted jets has been found to increase with target hardness. (See, for example, [3].) In this study we investigated two related technologies – one that employs cavitation and one that breaks the jet up into a series of slugs that produce water hammer type pressures upon impact. These technologies enable operation in both submerged and nonsubmerged conditions (such as when the well is blown down with compressed air).

1.2 The Geothermal Environment

We conducted a literature search in order to better understand the characteristics of the environment in which a geothermal well descaling tool will need to operate and the characteristics of various relevant scale types. The search included the databases of the Geothermal Resources Council (GRC) [4], the DOE Geothermal Energy Technical Site [5], DOE Energy, Efficiency and Renewable Energy Network Site [6], the Geothermal Energy Association [7], the International Geothermal Association [8], and the DOE Information Bridge [9]. In addition to information on scale formation and operating environment, a number of companies active in the geothermal drilling and production were identified.

Scale in geothermal wells forms due to a decrease in solubility of dissolved minerals such as calcium carbonate and silica. This can be due to temperature decrease or flashing of some of the water to steam. The latter often occurs due to depressurization of the geothermal fluid as it rises

in the well. The depth range over which scale forms varies with the geothermal site and the specific well at the site. As reported by [10], scale formation investigated at seven Dixie Valley well bores was found at depths between approximately 800 and 4,300 ft. The local ambient pressures, P_a, corresponding to these depths varies between approximately 350 and 1,900 psi.

2. DYNAJETS WaterJet Technologies

Cavitation is mainly known for its harmful effects, namely, loss of performance, erosion, and noise. The usual procedure to prevent these deleterious effects is to avoid the phenomenon by proper design and by limiting the operating conditions. However, attempts to induce and harness cavitation for useful purposes have been increasingly successful. Ultrasonic cavitation methods take advantage of the erosive power of cavitation for cleaning, emulsification, and mixing. In water jets, cavitation has for some time now been purposely induced in order to increase jet erosive power.

Experimental observations of submerged jets show the tendency of the turbulent eddies in their shear layer to organize in large structures. Excitation of a jet with periodic acoustic signals produced upstream of the nozzle by transducers or loud speakers shows a remarkable change of the jet structure into discrete ring vortices when the excitation frequency, f, matches the predominant natural frequencies of the non-excited jet. This corresponds to a Strouhal number, $S_{d,}$, close to 0.3 or one of its integer multiples. The Strouhal number is defined as

$$S_d = \frac{fd}{V}, \tag{1}$$

where V and d are the velocity and the diameter of the jet. This natural tendency of a submerged jet to organize into large structures is of great interest in aerodynamics for air jet studies. Crow and Champagne [11], and many others since, studied this phenomenon extensively and showed experimentally that forced excitation of the jet at the preferred frequency enhances the structuring. The vorticity is then mainly concentrated in ring-shaped large structures.

The potential of this phenomenon for submerged water jets was recognized and utilized to develop useful submerged jets having very high amplitude, periodic, oscillatory discharge without the use of moving parts in the supply system. (See, for example, [12-14].) The passive excitation is obtained hydroacoustically and structures the shear layer of the jet into discrete, well-defined ring vortices when the excitation frequency, f, matches the jet's preferred value. This can be obtained by feeding the final jet-forming nozzle with various types of acoustic chambers (for example, Helmholtz chambers or organ-pipe tubes) tuned to resonate at the desired frequency; and by shaping the nozzle so as to feed back the pressure oscillations which occur at the exit. Such devices are forms of "whistles" which self-excite and thus are totally passive. These jets are termed STRATOJET®s[1] and have shown enhanced erosivity from increased cavitation activity. The large pressure oscillations associated with the intensification of

[1] U.S. Patents: 4,262,757 4,389,071 4,474,251 4,508,577 4,681,264 4,716,849

cavitation, with resonance in the nozzle assembly, and with the production and disappearance of large vortical structures greatly improve the erosion and cleaning capabilities.

These self-resonating cavitating jets have shown large improvements over conventional jets in both cut depth and volume removal in selected laboratory settings and a range of cavitation conditions. The amount of improvement depends on the rock strength relative to the jet erosive strength, cavitation conditions such as the ratio between ambient pressure and jet pressure, and the ability to achieve resonance. The relative improvement in the cutting rate due to the introduction of cavitation increases with rock hardness, making this class of jets particularly attractive for use in medium to hard rock or scale. At deep depths, cavitation is suppressed in conventional jets. Self resonating jets produce cavitation for even higher ambient pressures thus enabling operation at deeper depths and producing good performance at lower nozzle pressures than conventional jets.

2.1 Principles of Operation of Self-Resonating Cavitating Jets

One possible type of STRATOJET® configuration is shown in Figure 1. It uses an organ-pipe acoustic chamber whose resonant frequency is selected to match the desired structuring frequency defined by the critical Strouhal number of the jet. This concept offers the simplest system design and has been used successfully for erosion studies and noise generation [13-17].

The principles of operation of an organ-pipe STRATOJET® are schematically represented in Figure 1. Two predominant sources of pressure fluctuations can be distinguished in addition to the classical unexcited turbulent shear layer between the jet and the surrounding liquid. One of these sources corresponds to the volume fluctuations of the moving vortex bubble rings formed in the center of the large structures of the self-excited jet. The other source of pressure fluctuations is more complex and relates to the exit area of the jet where high amplitude oscillations of the main flow characteristics are interrelated with the shear layer-nozzle lip interaction. The acoustic signals from both areas are forcing functions to the resonating chamber in the nozzle assembly. These signals strongly interact; they are both fed back and amplified by the organ-pipe.

Acoustic resonance is achieved in the nozzle feed-tube assembly when a standing wave forms in the "organ-pipe" section (length: L, diameter: D). Peak resonance will occur when the fundamental frequency of the organ-pipe is near the preferred jet structuring frequency. The exact resonance frequency is dependent on the contractions at each end of the organ-pipe, and the first mode resonance in the pipe will occur when the sound wavelength in the fluid is either two or four times L.

2.2 Effects of Jet Structuring on Cavitation Inception

The cavitation number is an important parameter in determination of the occurrence and behavior of cavitation phenomena. Thus all testing should be conducted under conditions that match the value(s) expected in practice.

The dimensionless parameter characterizing cavitation is the cavitation number, σ,

$$\sigma = \frac{P_a - P_v}{1/2\rho V^2}, \tag{2}$$

where P_a is the ambient or far field pressure, P_v is the vapor pressure of the liquid, ρ is the liquid density, and V is the characteristic velocity - the jet mean velocity. In deep wells, the ambient pressure is hydrostatic and directly related to hole depth. In the case of high-pressure submerged jets, $P_a >> P_v$, and for well-designed nozzles $1/2\rho V^2$ may be approximated by the pressure drop, ΔP, across the nozzle. Thus

$$\sigma \approx \frac{P_a}{\Delta P}. \tag{3}$$

The particular value at which cavitation is incipient is defined as

$$\sigma_i = (\frac{P_a}{\Delta P}) \text{ at inception.} \tag{4}$$

Thus if the operating conditions for a submerged jet are such that $\sigma/\sigma_i < 1$, cavitation will occur, and as σ/σ_i continues to decrease below unity the amount of cavitation will increase. When a cavitating jet impinges against a surface, the cavities formed in the jet collapse on that surface and produce very high local pressures and very high speed microjets. (As an example, Figure 2 presents the results of a numerical simulation we conducted of high speed microjet formation on bubble collapse. Shown are a close up of the microjet and the resulting velocity field.) The resulting pressures are much greater than the jet stagnation pressure ($1/2\rho V^2$), and the resulting cleaning or cutting action is substantially greater than when the jet is not cavitating. A great advantage of the STRATOJET® class of jets is an increase in σ_i over conventional jets by a factor of 3 with current designs. The ability to achieve cavitation at high ambient pressures is of particular importance to deep well operations. *Self resonating jets produce cavitation for much higher ambient pressures than conventional jets thus enabling operation at deeper depths* and producing better performance at lower nozzle pressures than conventional jets.

The increase in σ_i is due to the decreased pressures at the core of the structured vortices generated. The resulting vortex ring cavities can be seen in Figure 3. This figure presents a strobe photograph from a large scale visualization study at a value of σ=0.21.

For the scale depth conditions at Dixie Valley [10] noted above, the cavitation number ranges between 0.07 and 0.38 for a jet operating pressure of ΔP = 5,000 psi.

2.3 Self-Resonating Pulsed Jet Technology

The SERVOJET® jet system is also an acoustically self-resonating jet originally developed to generate water "slugs" or drops at known frequencies and to operate in non-submerged conditions - i.e., in air. Interrupted liquid jets have been proven to be advantageous over steady jets due to their large water hammer type impact pressures. Details of our development of self-resonating interrupted water jets can be found in [18]. In a submerged condition, it operates

similar to the STRATOJET® and structured cavitation is generated in the shear layer created between the high speed water jet slugs and the surrounding liquid. However, the STRATOJET® configuration is usually preferred since it involves fewer flow contractions and expansions and thus less pressure losses and little interaction with the working fluid. In air jet erosivity is improved by jet interruption leading to slug and drop production.

3. EXPERIMENTAL SETUP AND PROCEDURES

3.1 Test Facility

Experiments were conducted in DYNAFLOW's High Pressure Cell (HPC) capable of ambient pressures up to approximately 2800 psi. A photograph of the HPC is presented in Figure 4. The HPC is a cylindrical pressure vessel with inside dimensions of approximately 9.5 inch diameter and 28 inch length with three quartz view ports circumferentially spaced and located near its mid length. Constructed for studies of deep hole drilling with cavitating jets, it includes a fixture in which rocks are placed and rotated at various speeds for cutting beneath the jet. Another fixture enables the rock to advance at a controlled rate towards the nozzle thus enabling actual drilling. This capability was employed in experiments described below with multiple orifice nozzles. The rock surface being cut can be viewed from the view ports. Ambient pressure is adjusted and maintained by a choke plate which acts as a back pressure valve in the outflow line. The jet flow is driven by a Weatherford five piston positive displacement pump capable of up to 20 gpm at 10,000 psi or 11 gpm at 20,000 psi.

Nozzle acoustic resonance was checked with Piezotronics 101-A04 pressure transducers (5 mv/psi sensitivity) located in the HPC wall and used to measure the fluctuating component of the pressure, P'. The output of the transducer was monitored with both a digital rms meter to obtain the rms value of the fluctuating pressure component and a spectral analyzer to ascertain the frequency content of the fluctuations and determine the peak (resonant) frequencies of the nozzles. These measurements were used to determine whether or not a particular self-resonating nozzle has achieved good acoustic resonance - an important factor in achieving good performance. The organ-pipe length for the self-resonating nozzle was "tuned" to the jet exit velocity (i.e., to ΔP).

3.2 Target Materials and Characteristics

In order to carry out meaningful laboratory tests of scale removal, an appropriate target material needs to be employed. Ideally, actual scale should be used as the target material. This, however, has several problems associated with its use. It requires removal and transportation of the scale from its source – a geothermal well site – and storage under conditions that do not affect its mechanical properties. This includes maintenance of a wet environment. In addition, actual field generated scale involves inherent sample to sample variability due to both potential local inhomogeneities and differences between samples taken from different locations and acquired at different times. A similar problem arises in tests of rock cutting by water jets. Depending on the rock type, substantial sample to sample variation can be found due to local composition variation and flaws as well as bedding plane orientation. For this reason, such samples are always tested in

the same orientation in which they were cut from the formation. We have found for rock that use of a more repeatable and uniform property material as a target material for initial development and screening of designs is desirable. We have utilized man-made simulated rock and aluminum plate (6061-T6) for this purpose with great success [3].

In the current project, initial development and screening was conducted with simulants. A set of samples made of cement (sand, but no aggregate) was investigated. Two types – a "quick-set" and a fiber reinforced cement were selected for further evaluation.

In order to assess the effect of cure time on the hardness of these simulants, a series of tests were conducted on 2 in. thick samples of both fiber-reinforced and quick-set cements. Repeated cuts of each sample were performed for a series of increasing cure times between 3 and 7 days. For these tests, the samples were submerged, and a 0.053 in. diameter conventional jet (Spraying Systems Washjet ¼ MEG 0005) operating at 5,000 psi and 5.4 gpm was translated across the surface at 1 in/s and at a 1 in. standoff. As can be seen in Figure 5, the results show a continuing decrease in measured cut depth with time indicating a continued increase in hardness that is significant. For the top of the fiber reinforced cement the cut depth varied from 0.31 in. at 3 days cure to 0.085 in. for 7 days cure time. Similar variations with cure time were found on the other sample surfaces tested. The top surface of the fiber-reinforced cement was found to be consistently the hardest. The cut depth in the fast set sample was approximately 40% greater than that in the bottom of the fiber reinforced indicating an approximately 40% greater cutting resistance for the fiber reinforced cement. Based on these results, we determined that to achieve sample uniformity we needed to control and/or adjust for the cure time. We thus endeavored to test samples with cure times of approximately 3 days and to conduct comparison tests head-to-head on the same samples.

Samples of silica and calcium carbonate geothermal scale were obtained from CalEnergy courtesy of Mr. Paul Spielman [19]. We have performed cutting tests on these samples to compare them under the same conditions with the various simulants. The comparison tests were conducted with a 0.034 in diameter SERVOJET® operating at 5,000 psi, 1.5 gpm and translating across the sample at various speeds between 0.5 and 2 in/s at a standoff of 2.25 in. (66 diameters). The tests were conducted submerged at atmospheric ambient pressure. The results are summarized in the following table:

Material	Erosion Depth/Width (in.) at Various Translation Velocities		
	0.5 in/s	1 in/s	2 in/s
Calcium Carbonate	0.125/0.5		Onset (pecking)
Silica	Onset (pecking)	0	0
Fast Set Cement	0.11/0.78		
Fiber Reinforced Cement	Onset (0.025 in depth)	0	0

The calcium carbonate experienced the onset of damage – a surface pecking - at 2 in/s while sustaining a cut 0.125 in deep and 0.5 in wide at 0.5 in/s. The harder silica exhibited no damage at 2 and 1 in/s while sustaining the onset of damage at 0.5 in/s. Similar results were produced in the top surfaces of a fast set and a fiber reinforced cement, respectively. At 0.5 in./s, the fast set exhibited a cut 0.11 in deep cut 0.78 in wide while the fiber reinforced experienced the onset of

erosion with a depth of about 0.025 in. Based on these data, the fiber reinforced cement (top surface) was selected to simulate silica and the fast set cement selected to simulate calcium carbonate. The silica, being the harder scale, and its fiber reinforced cement simulant, were the primary focus of testing.

4. SIMULATED SCALE EROSION TEST RESULTS

In order to assess jet performance under downhole conditions, cutting tests were conducted in our High Pressure Cell on samples of fiber reinforced cement. Three jet types designed to operate at comparable flows and pressures were employed: a conventional jet, a self-resonating organ pipe STRATOJET®, and a self-resonating SERVOJET® employing a combination of organ pipes and a Helmholtz chamber. (Both the STRATOJET® and the SERVOJET® were designed to induce structured cavitation.)

In order to assess the best pressure at which to test the cavitating resonating STRATOJET®, the rms pressure fluctuations were measured as the pressure drop was varied for a constant value of the cavitation number (σ = 0.3). These data are plotted in Figure 6. As can be seen, the pressure fluctuations normalized by pressure drop across the nozzle show two local maxima - at pressure drops of 2,000 and 6,000 psi. Based on this, ΔP = 6,000 psi was chosen as the operating pressure for performance evaluation.

Both cut depths, h, and diameters, w, were measured. Nominal volumes, $\mathcal{V}$, were calculated by assuming a cylindrical cut hole whose volume is given by

$$\mathcal{V} = \pi w^2 h/4. \qquad (5)$$

At a 1 in. standoff (X_{so}/d_o = 19) and P_a = 500 psi, ΔP was increased until the onset of erosion of the sample. For the conventional jet, this occurred for 180 sec exposure at ΔP = 5,000 psi and 50 sec exposure at ΔP = 6,000 psi. A series of tests varying the ambient pressure, standoff, and exposure time was then conducted for the three jet types at ΔP = 6,000 psi. A similar evaluation was performed under non-submerged conditions – "in air".

4.1 Influence of Ambient Pressure

Figures 7-9 present the measured cut depths, h, as functions of time for up to 120 sec exposure for the three jet types at a 1 in. standoff (X_{so}/d_o = 19) and ambient pressures of 150, 300 and 500 psi (σ = 0.025, 0.05, 0.083), respectively. The strong influence of cavitation number or ambient pressure is apparent with an order of magnitude variation in the cut depths between ambient pressures of 150 and 500 psi. The STRATOJET® run at P_a = 150 psi was stopped after only 10 sec due to it cutting through nearly the entire 2 in. thickness of the sample. These data show that the STRATOJET® significantly outperforms the other two nozzle types at all three ambient pressures. The SERVOJET® employed is better than the conventional jet at P_a = 150 psi, about the same at P_a = 300 psi, and poorer at P_a = 500 psi.

The corresponding average hole diameters, w, and nominal volumes, $\forall$, (as calculated from relation (5)) are presented in Figures 10-13. As can be seen, the variations in diameter and volume are much less than the variations in depth. The diameters are also seen to change very slowly with time after an initial period. The relative rankings of the three jet types are the same for width and volume as for depth. The STRATOJET® is clearly the best performer over the entire range investigated. It should be noted that at P_a = 150 psi, the SERVOJET® produces a cut volume approximately twice that of the conventional nozzle.

4.2 Influence of Standoff

Figures 14-16 present the influence of standoff at a P_a = 150 psi (σ=0.025). Again, the STRATOJET® has the largest cut depths at all three standoffs. This is followed by the SERVOJET® at 1 and 2 in. standoffs At a 3 in. standoff neither the conventional nor the SERVOJET® produced a measurable cut depth after 120 sec. The STRATOJET® was also found to produce the largest diameters (Figure 15) and volumes (Figure 16) at all three standoffs. It is clearly the preferred jet for operation at these conditions.

4.3 In-Air Tests

Figures 17-19 present, respectively, the cut depths, diameters, and nominal volumes for operation of the three jet types in air (not submerged) at atmospheric pressure at standoffs of 1, 2, and 3 inches. In terms of depth, the STRATOJET® at a 1 in standoff is the best performer. There are three cases with cut depths comparable to each other – the STRATOJET® and SERVOJET®at a 2 in standoff and the conventional jet at a 3 in. standoff. The best standoff for the conventional jet for cut depth is 3 in. It should also be noted that the SERVOJET® exhibits a cut depth at a 2 in standoff approximately twice as large as that cut at 1 or 3 in standoffs indicating an optimal standoff of approximately 38 nozzle diameters. However, the SERVOJET® produces a cut diameter significantly larger than either of the other two jets. At standoffs of 2 and 3 in, its cut diameter is 3.5 times that of the conventional jet, while it is twice that of the conventional jet at a 1 in standoff. The STRATOJET® cut diameters fall in between those of the SERVOJET® and the conventional jet. The largest cut volumes are created by the SERVOJET® at 2 and 3 in standoffs followed by the STRATOJET® at a 1 in standoff (Figure 19).

5. MULTIPLE JET CONFIGURATION TESTS

Based on results described above for the three nozzle types, the STRATOJET® was selected for further investigation. In order to provide a means of expanding the coverage area and increasing the volume removal rates – important to practical systems – we investigated the potential of multiple orifice designs. To that end, we designed, fabricated, and tested two multi-orifice STRATOJET® nozzles. A photograph of these is presented in Figure 20. Figure 21 provides a sketch of the two configurations. Each has 7 individual orifices including a central orifice and six equally spaced orifices arranged in a circular pattern about the central orifice. The complete set of 7 orifices is fed from a common organ pipe that also acts as a common acoustic amplifier to drive the jet resonance.

The nozzle end in which the orifices are located has a hemispherical shape. The centerlines of all 6 outboard orifices are at a common angle, β, to the axis of the nozzle and the centerline of the center orifice. The centers of the 6 outboard orifices are equally spaced along a circle surrounding the central orifice and having a radius R measured perpendicular to the nozzle axis. A conical pattern is then formed by the jets from the outer ring of 6 orifices with the central jet traveling along the axis of this cone. In each configuration, some modification of orifice diameters was performed based on results. Two basic configurations, distinguished by their value of β, were tested. Configuration I (β=35°) was a wide pattern producing a large diameter footprint. Configuration II (β=18°) was a narrow pattern producing a smaller diameter footprint, but one in which the craters from the individual jets merged to form a single large crater. The details of the various configurations are listed in the following table.

Configuration	**Center Orifice Diameter**	**Outboard Orifices Diameter**	β	R	ΔP	Q
	(in)	(in)	(degrees)	(in)	(psi)	(gpm)
I-A	0.023	0.038	35	0.128	6000	16.7
I-B	0.030	0.038	35	0.128	5600	19
II-A	0.030	0.036	18	0.1	6000	13.4
II-B	0.030	4 0.036 & 2 0.038	18	0.1	6000	14
Single Orifice	0.094	--	--		6000	17.5

Results were compared with those obtained with a single orifice operating at the same pressures and sized to have a similar flow rate.

In order to address a very hard scale, dolomite and limestone were used as target materials. In addition to ascertaining that resonance was achieved, three types of experiments were performed:

- Visualization and observation to assure that cavitation rings were being produced from all the orifices; that the individual jets were not experiencing adverse interference with each other; and to determine the standoff over which the ring cavities persisted.
- Static tests in which jetting took place at a fixed location for a specified time period.
- Advancing tests in which the entire nozzle assembly advanced into the target through the crater created by the jet tool.

Based upon initial visualization experiments, a jet standoff of 0.25 in was selected, and a set of static tests conducted in dolomite with an exposure time of 60 sec in order to evaluate the cut pattern. Configuration I-A was run at ΔP = 6,000 psi and P_a = 1,000 and 300 psi (σ = 0.17 and 0.025). At P_a = 1,000 psi, the pattern consisted of 7 separate craters due to the 7 orifices that were nearly touching, but that did not form a common crater. At P_a = 300 psi, the individual craters partially merged, but did not completely remove the dolomite between individual craters.,

particularly around the central cut. To address this, the central orifice size was increased to obtain Configuration I-B, and the initial standoff was decreased to 0.125 in. The increase in orifice size proved slightly too large for our pump, and the test was conducted at ΔP = 5,600 psi, P_a = 300 psi. This did, however, produce the desired merging of the individual craters into a common crater of 0.88 in diameter and 0.14 in depth. For comparison, a single orifice was operated at comparable total flow, pressure, standoff, and exposure time. It produced a crater of 0.98 in diameter but only 0.045 in deep. Clearly, the multi-orifice design was superior.

Based on this experience, a new design with a smaller angle between the jets was tested – Configuration II-A. An initial cutting test with this design exhibited some imbalance between the cutting of the various outboard orifices (probably due to some small fabrication irregularities). Thus the diameter of two orifices were increases a small amount to obtain Configuration II-B. A 60 sec static test of this nozzle in dolomite (0.25 in standoff, ΔP = 6,000 psi, P_a = 300 psi) produced a good common crater with a 0.78 in diameter and a 0.26 in depth.

The last set of experiments was conducted to assess the ability of such a multi-orifice tool to be employed in practical situations of substantial scaling. It demonstrated the ability to bore through even very hard substances without need of mechanical assist. The ability to advance depends on the ability to create a large enough diameter crater to accommodate the tool diameter and a removal rate rapid enough to accommodate the advance rate of the nozzle. Thus, at very high advance rates, the crater width and depth will not be large enough to allow the nozzle assembly to pass and the tool will contact the target material and "stall." One would like to operate at the highest speed possible without experiencing stalling in order to minimize rework costs and the time that the well is offline. In these experiments, the maximum diameter of the tool was 0.70 in at a specially fabricated upstream coupling. (See Figure 20.)

These nozzle advancing tests were performed with limestone samples 3 inches thick and 6 inches square in the transverse direction with configuration II-B. (The switch was made from dolomite to limestone since the dolomite samples available were of insufficient thickness to evaluate advancement of the nozzle.) An initial 30 sec static test in limestone (0.25 in standoff, ΔP = 6,000 psi, P_a = 300 psi) confirmed the results in dolomite producing a crater 0.95 in wide by 0.38 in deep. Experiments were then conducted at different advance rates.

Figure 22 presents a plot of the penetration depths achieved (prior to stalling) at various advance rates in limestone. A penetration depth of 3 in. represents a cut through the entire thickness of the limestone block without stalling. Jetting began with an initial standoff of 0.25 in. The ambient pressure was 300 psi, and thus σ = 0.05. In two of these experiments (one each at advance rates of 10 and 12 in/min) a problem with the test cell mechanical drive resulted in stoppage of the advance just short of 2 in. These are marked on 22. Neither of these two runs nor the run at 6 in/min stalled. The latter produced a successful advance through the entire sample thickness. Based on these data, the maximum advance rate (without stall) with this particular configuration is between 6 and 10 in/min. Also shown in 22 are the average diameters of the craters produced and the outer dimension of the coupling, which must fit through the hole (0.70 in). Although all the average crater diameters are larger, the craters are somewhat irregular and, in order to advance, the smallest dimension of the crater must always be somewhat larger than the coupling. Based on these data, this requires a mean diameter of about 0.9 in.

The complete advancement at 6 in/min and the significant penetration depths prior to stalling at higher advancement rates indicate that this type of multi-orifice design with cavitating water jets is very promising for pure water jet removal of hard scales as well as rock.

6. CONCLUSIONS

Improved methods of removal of hard scale from geothermal wells were investigated. Experiments were conducted utilizing both actual and simulated scale with three classes of water jets: cavitating self-resonating STRATOJET® and SERVOJET®, and a conventional jet operating at the same conditions under both submerged and "in-air" conditions for a range of standoffs and ambient pressures. Under submerged conditions, the STRATOJET® was found to produce the largest cut depths and volumes. Volume increases of as much as a factor of 25 over the conventional jet were measured. Under "in-air" conditions, the STRATOJET® produces the deepest cut and largest volume at a standoff of 19 diameters (1 in). However, at larger standoffs, the larger SERVOJET® "footprint", due to the generation of discrete water slugs, results in a volume removal three to five times that of the other jets with a maximum removal rate at a 39 diameter standoff (2 in).

Based on the results of the single orifice experiments, a 7 orifice STRATOJET® nozzle tool was developed and evaluated. The tool was found capable of advancing through limestone at rates in excess of 6 in/min at ΔP = 6,000 psi with no additional mechanical assistance. Such a tool design could be utilized to cut through heavily scaled wells in which the extent of the scale renders passage of large sized tools impossible.

7. REFERENCES

1. Glowka, D., ``Recommendations of the Workshop on Advanced Thermal Drilling," Sandia National Laboratories Technical Report SAND97-2903, December 1997.

2. De Rocher, T. and Shevenell, L., ``Calibration and Testing of the Brine Chemistry Models GEOFLUID and TEQUIL at Nevada Geothermal Resources," U.S. DOE Geothermal Technical Site Research Summary (http://geotherm.inel.gov/fy95), fiscal year 1995.

3. Chahine, G. L., Kalumuck, K. M., and Frederick, G. S., "Cavitating Water Jets for Deep Hole Drilling in Hard Rock," Proceedings, 8th American Water Jet Conference, Houston, TX, August 1995.

4. http://www.geothermal.org

5. http://geothermal.id.doe.gov.org

6. http://www.eren.doe.gov

7. http://www.geotherm.org

8. http://www.demon.co.uk/geosci/igahome.html

9. http://www.doe.gov/bridge

10. Benoit, W. R., "Early Stage Carbonate Scaling Characteristics in Dixie Valley Wellbores," Transactions, Geothermal Resources Council, vol. 11, October 1987.

11. Crow, S. and Champagne, T., "Orderly Structure in Jet Turbulence," *Journal of Fluid Mechanics,* vol. 48, August 1971.

12. Chahine, G. L., Genoux, Ph. F., and Liu H.L., "Flow Visualization and Numerical Simulation of Cavitating Self-Oscillating Jets," *7th International Symposium on Jet Cutting Technology*, Ottawa, Canada, June 1984.

13. Chahine, G. L., Genoux Ph. F., Johnson, V. E. Jr., and Frederick, G. S., "Analytical and Experimental Study of the Acoustics and the Flow Field Characteristics of Cavitating Self-Resonating Water Jets," *Sandia National Laboratories, Albuquerque, NM, Contractor Report SAND84-7142*, September 1984.

14. Chahine, G. L. and Johnson, V.E. Jr., "Mechanics and Applications of Self-Resonating Cavitating Jets," *Proceedings of the International Symposium on Jets and Cavities, ASME, WAM*, Miami, FL, November 1985.

15. Chahine G.L., Genoux Ph. F., Liu, H. L., and Johnson V.E. Jr., "Analytical and Experimental Study of Self-Resonating Jets: Nozzle-Jet and Wall-Jet Interactions," *Sandia National Laboratories, Albuquerque, NM, Contractor Report SAND86-7124*, September 1986.

16. Johnson, V. E., Jr., Chahine, G. L., Lindenmuth, W. T., Conn, A. F., Frederick, G. S., and Giacchino, G. J., "Cavitating and Structured Jets for Mechanical Bits to Increase Drilling Rate, Part 1: Theory and Concepts; Part 2: Experimental Results," *Journal of Energy Resources Technology,* vol.106, June 1984.

17. Chahine G. L., Johnson V.E. Jr., Kalumuck K.M., Perdue T.O., Waxman D.N., Frederick G.S., and Watson R.E., "Internal and External Acoustics and Large Structures Dynamics of Cavitating Self-Resonating Water Jets," *Sandia National Laboratories, Albuquerque, NM, Contractor Report SAND86-7176*, July 1987.

18. Chahine G. L., Conn, A., Johnson, V., and Frederick, G., "Passively Interrupted Impulsive Water Jets," *6th Intl. Conf. on Erosion by Liquid and Solid Impact*, Cambridge, U.K., Sept. 1983.

19. Mr. Paul Spielman, Resource Department, CalEnergy Company, Inc., 900 N. Heritage Bldg. D, Ridgecrest, CA 93555.

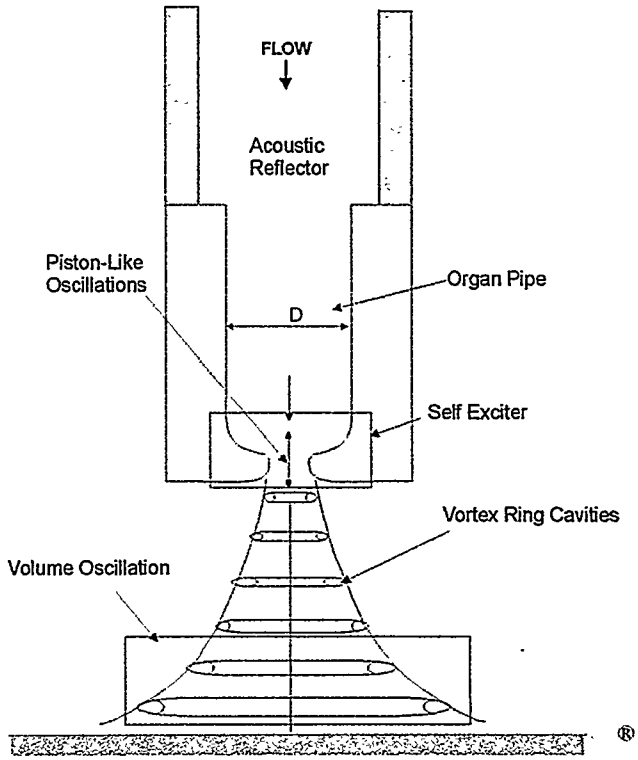

Figure 1. Schematic of Principles of Operation of an Organ-Pipe STRATOJET®

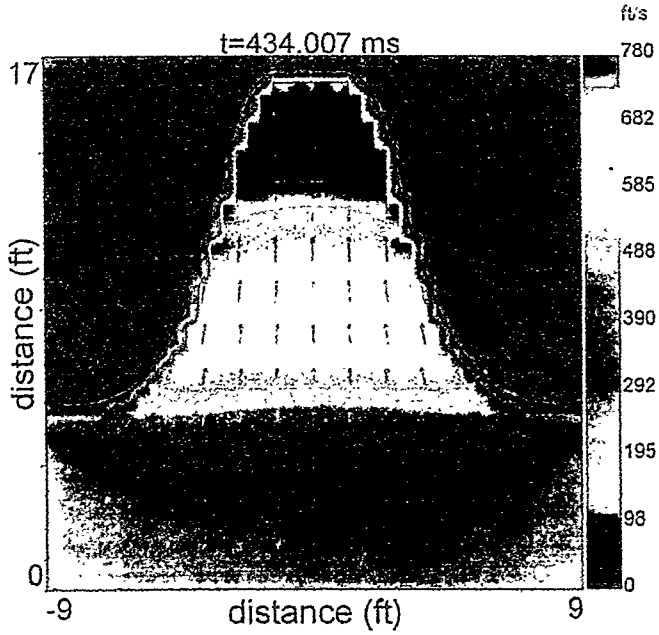

Figure 2. Results Of Numerical Simulation Of Bubble Collapse And Formation of High Speed Microjet at an Ambient Pressure of 2500 psi Using DYNAFLOW's 3D Code, 3DYNAFS. Shown are Computed Velocity Vectors and Contours.

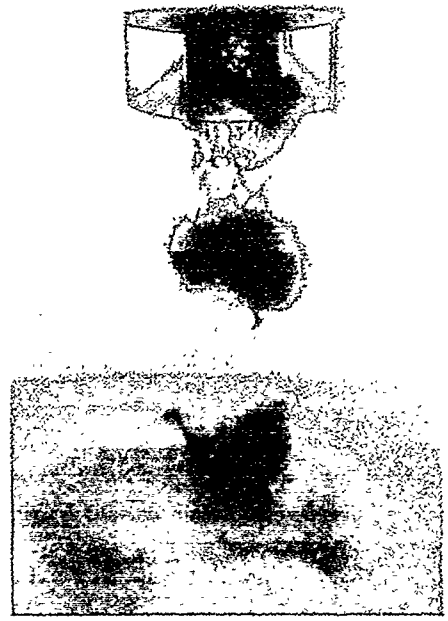

Figure 3. Visualization of a Large Scale STRATOJET®. $\sigma = 0.21$.

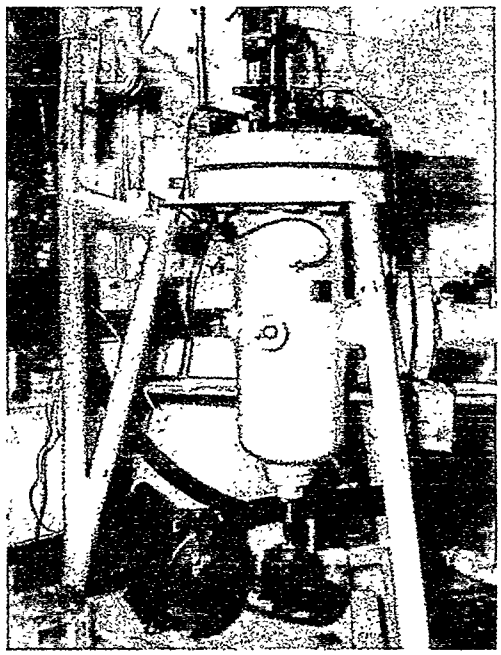

Figure 4. DYNAFLOW's High Pressure Cell (HPC) Capable of Ambient Pressures Up to 2800 psi.

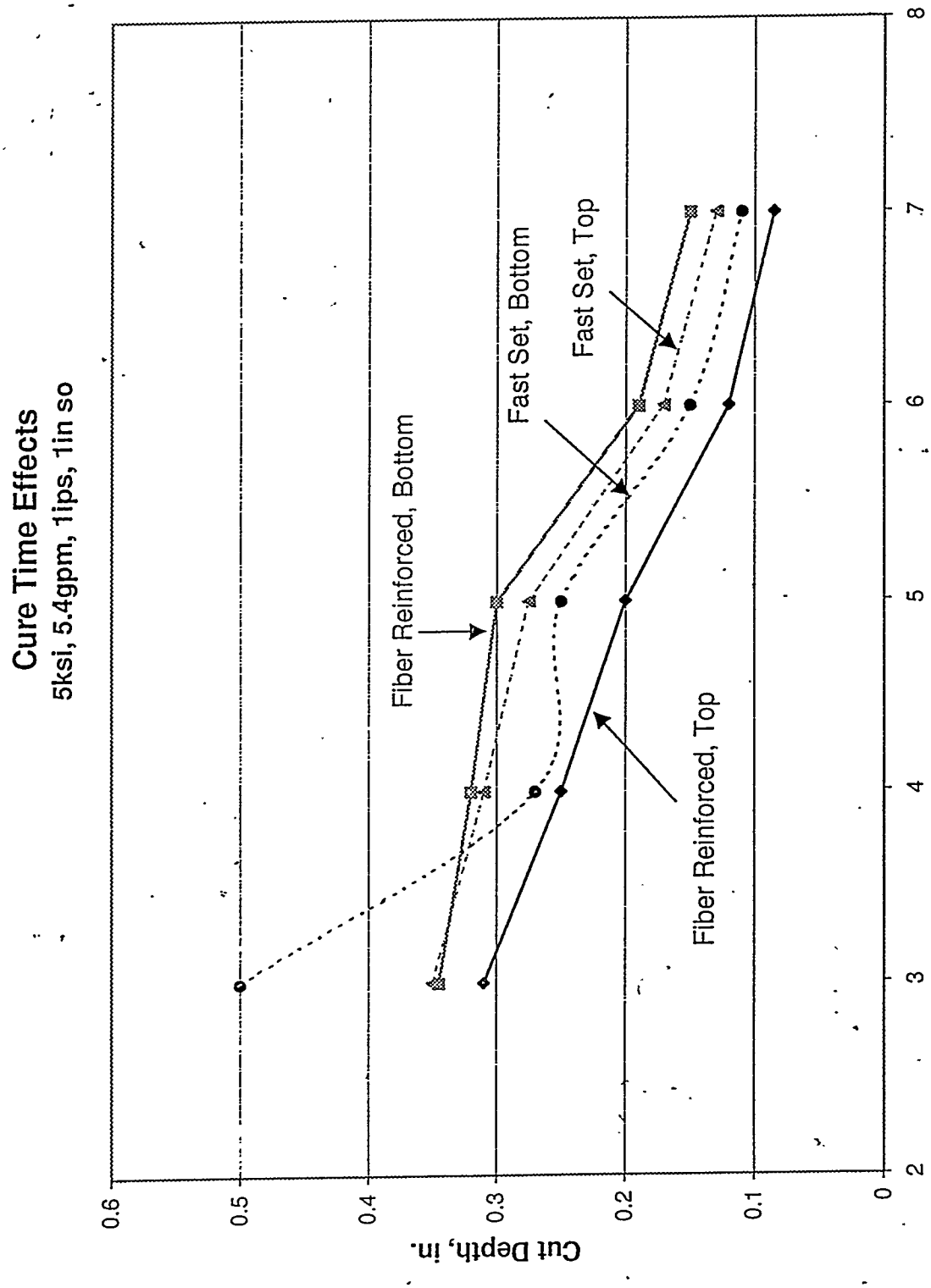

Figure 5. Influence of Cure Time of Laboratory Cement Samples on Cut Depth.

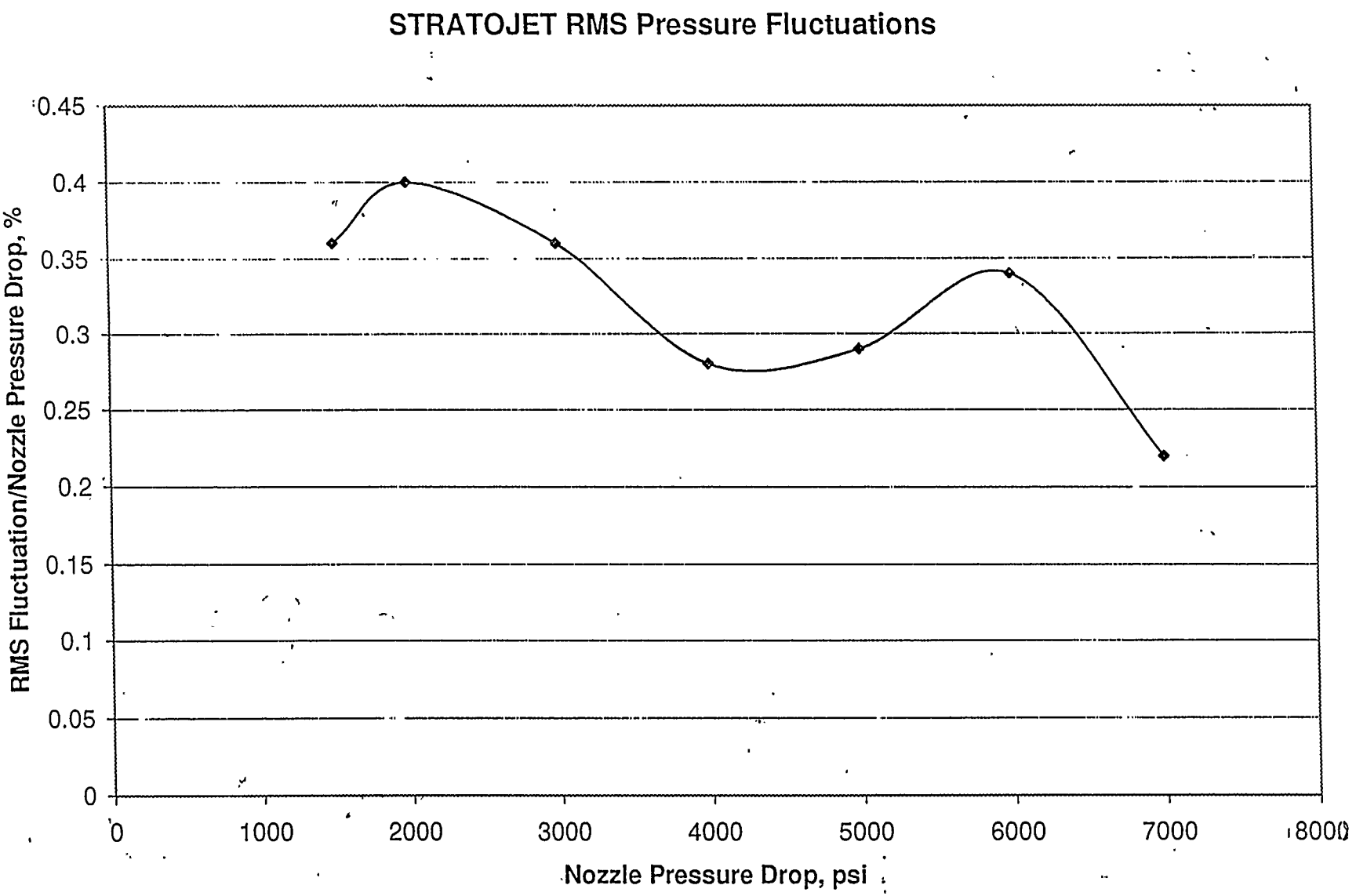

Figure 6. Normalized RMS Fluctuating Pressure $P'/\Delta P$ vs. Nozzle Pressure Drop ΔP for STRATOJET® Nozzle at a Constant Value of Cavitation Number $\sigma = 0.3$.

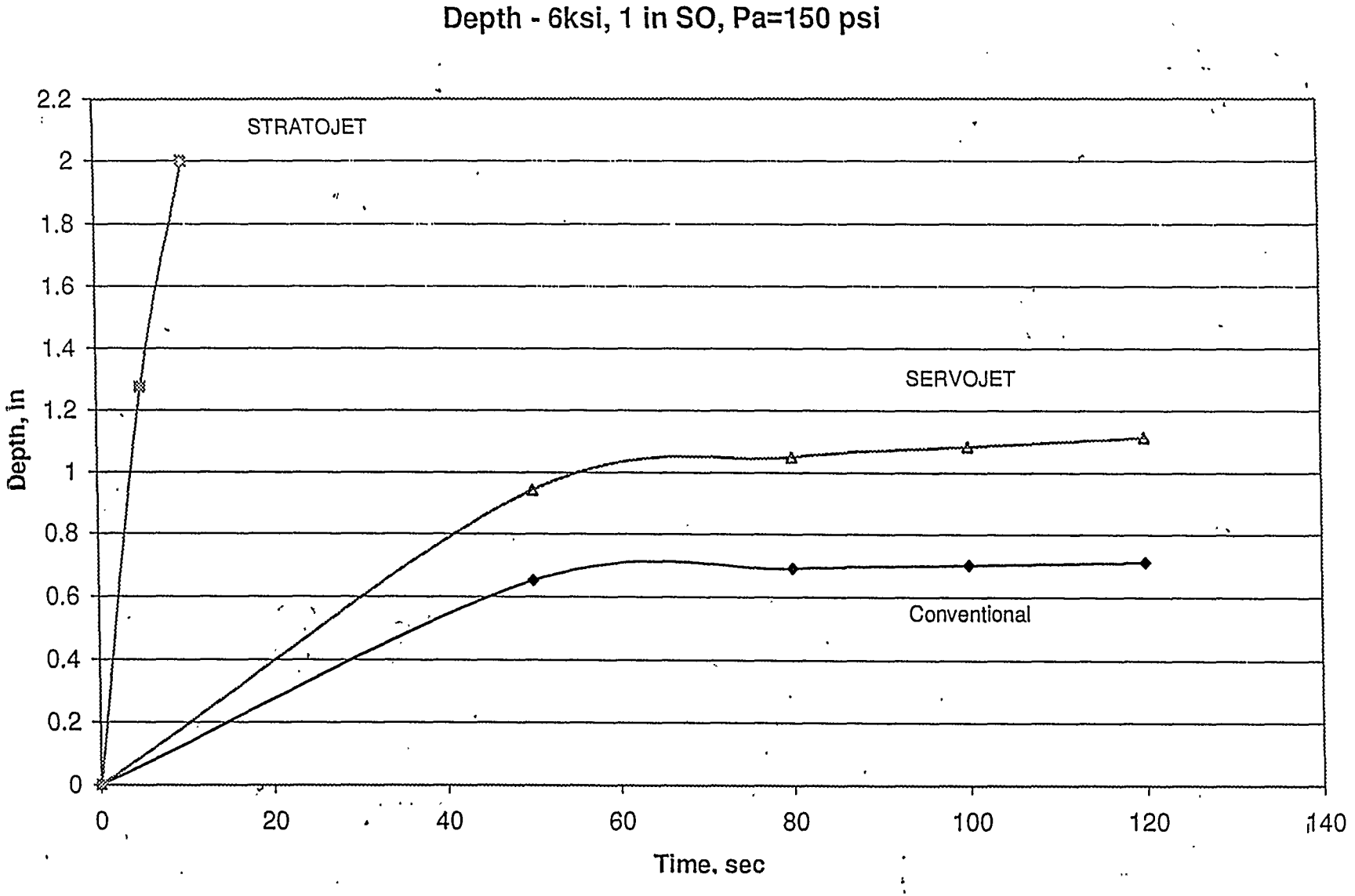

Figure 7. Progression of Depth of Erosion with Time for Three Nozzle Types at an Ambient Pressure of 150 psi. Standoff = 1.0 in., ΔP = 6,000 psi, Flow Rate = 5.9 gpm.

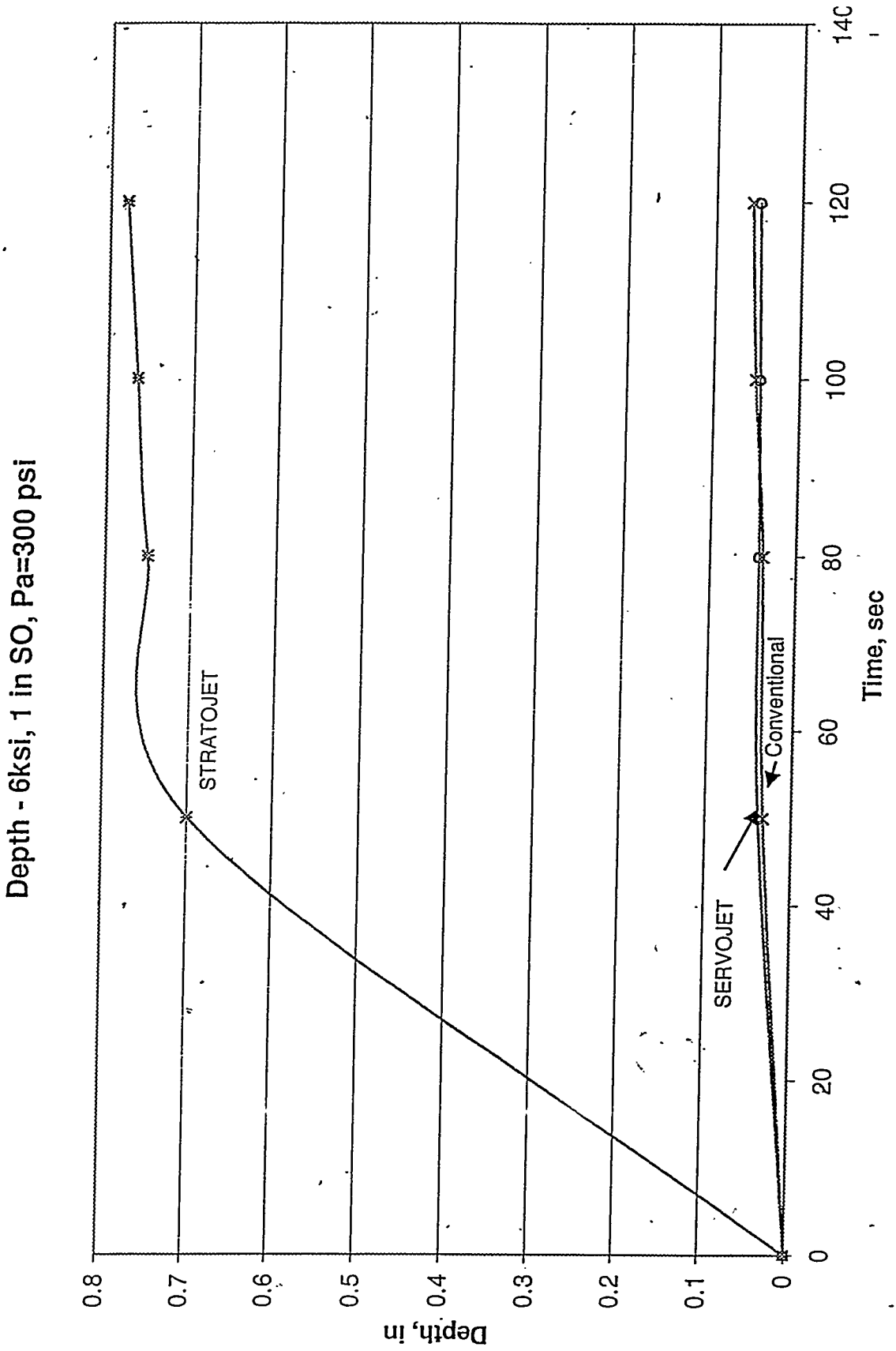

Figure 8. Progression of Depth of Erosion with Time for Three Nozzle Types at an Ambient Pressure of 300 psi. Standoff = 1.0 in., ΔP = 6,000 psi, Flow Rate = 5.9 gpm

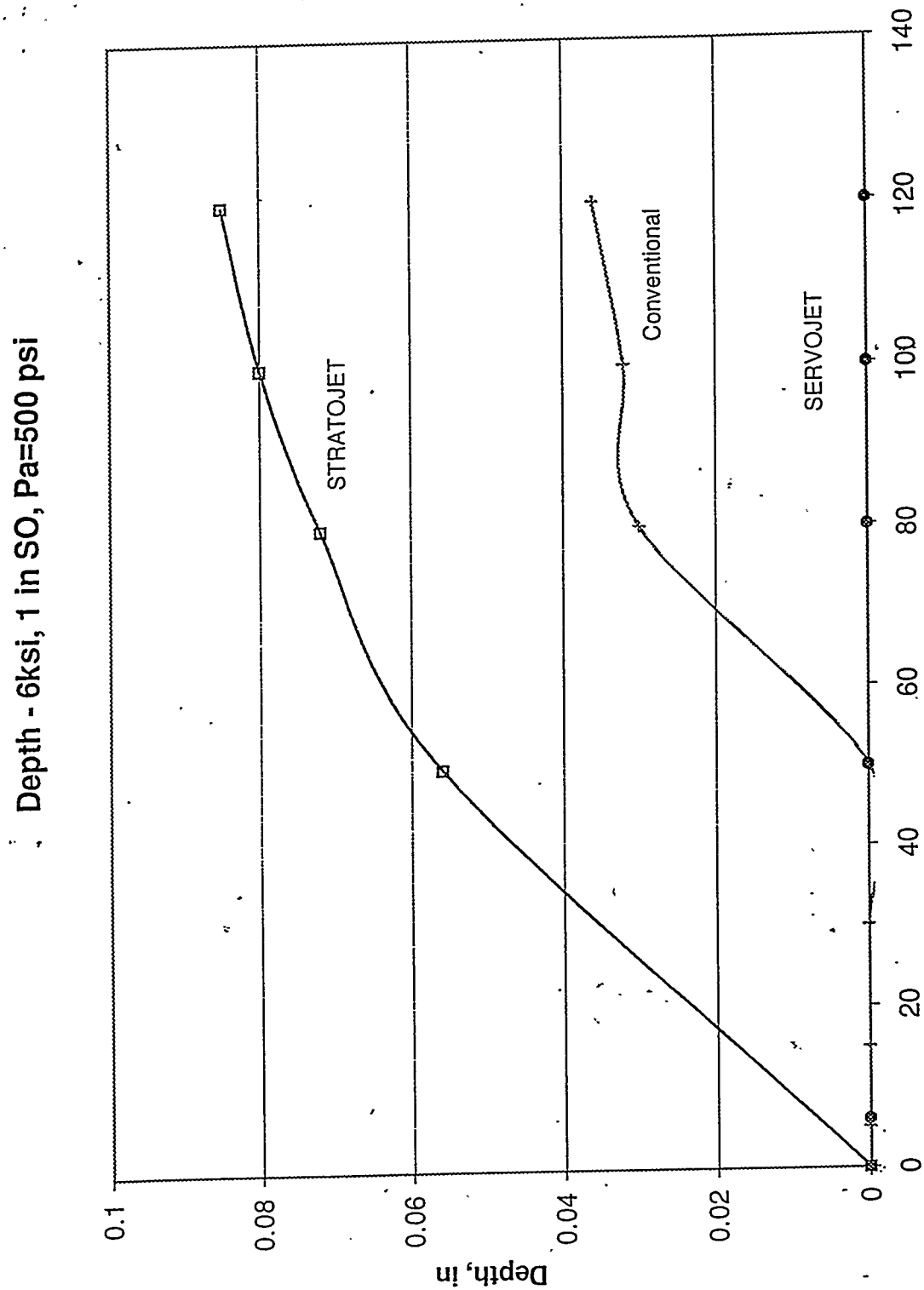

Figure 9. Progression of Depth of Erosion with Time for Three Nozzle Types at an Ambient Pressure of 500 psi. Standoff = 1.0 in., ΔP = 6,000 psi, Flow Rate = 5.9 gpm.

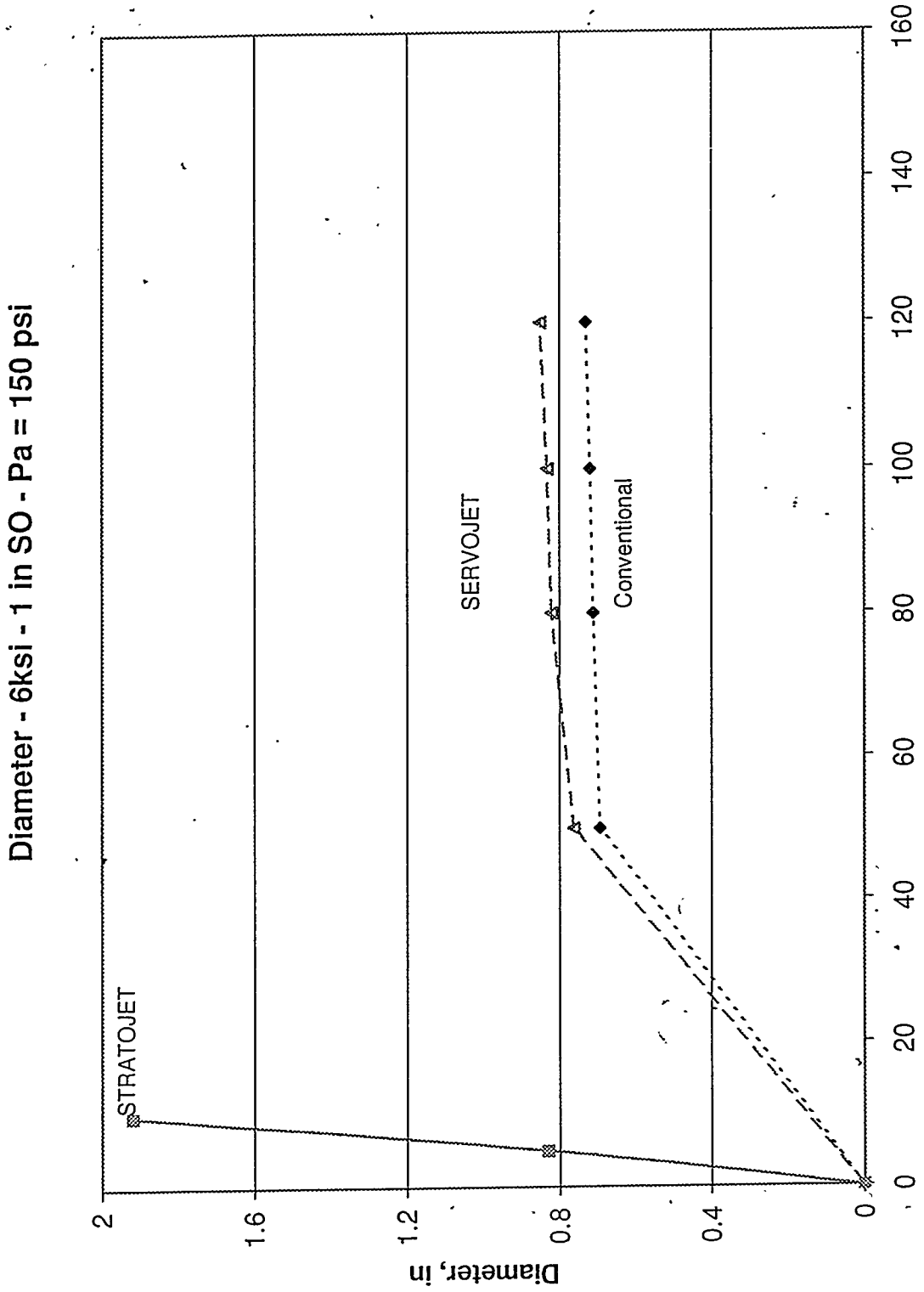

Figure 10. Progression of Diameter of Erosion with Time for Three Nozzle Types. Standoff = 1.0 in., ΔP = 6,000 psi, P_a = 150 psi, Flow Rate = 5.9 gpm.

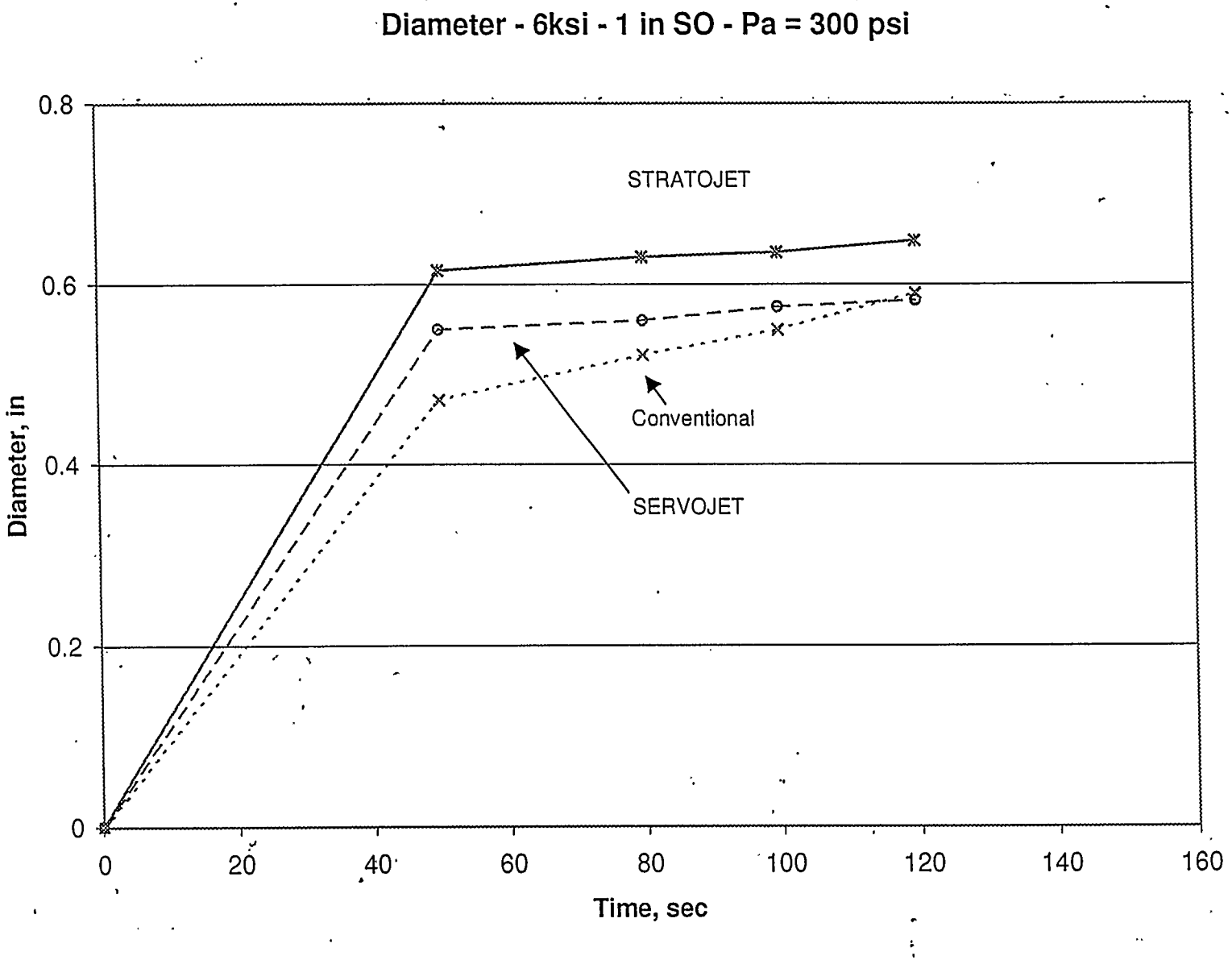

Figure 11. Progression of Diameter of Erosion with Time for Three Nozzle Types. Standoff = 1.0 in., ΔP = 6,000 psi, P_a = 300 psi, Flow Rate = 5.9 gpm.

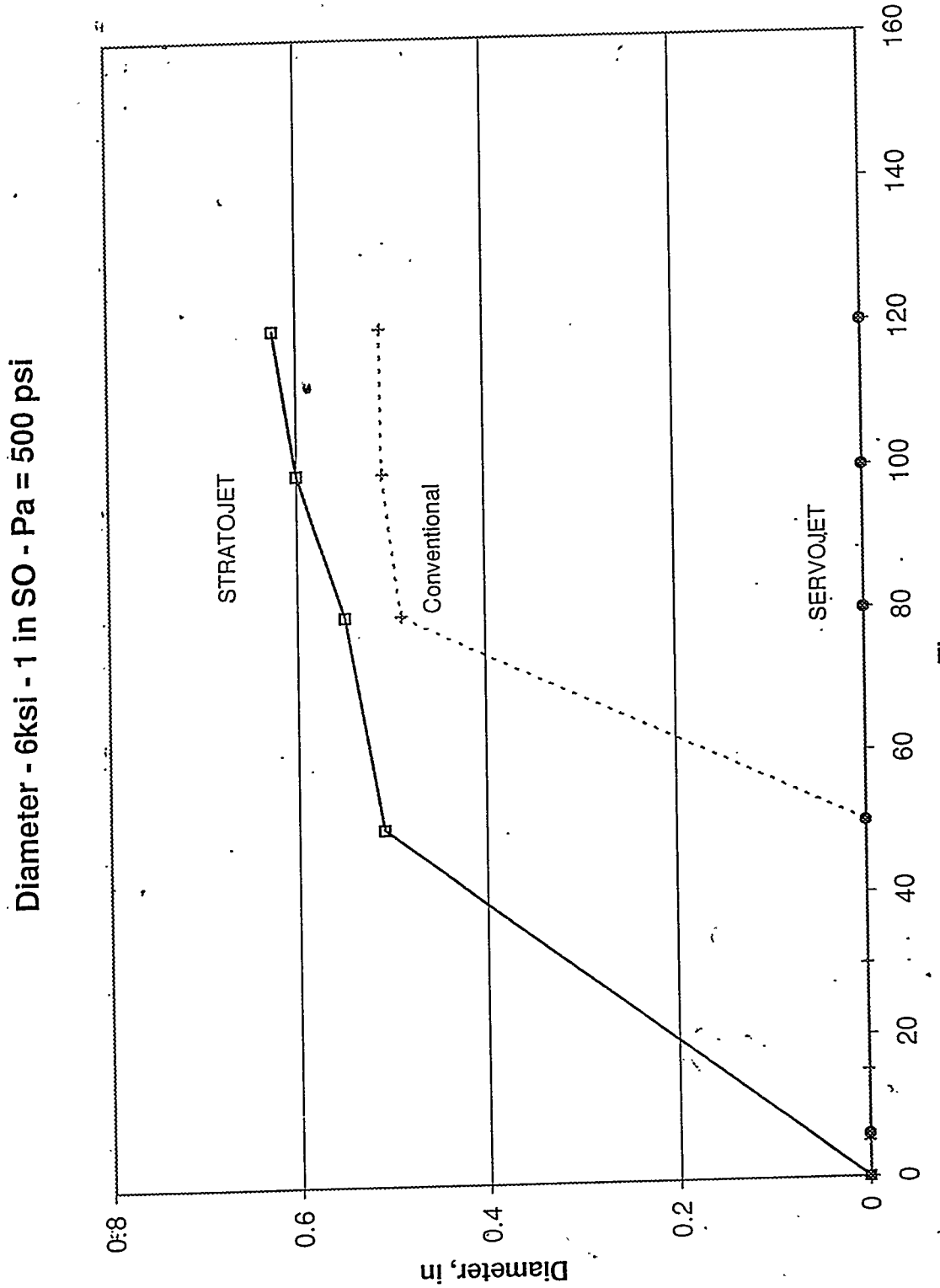

Figure 12. Progression of Diameter of Erosion with Time for Three Nozzle Types. Standoff = 1.0 in., ΔP = 6,000 psi, P_a = 500 psi, Flow Rate = 5.9 gpm.

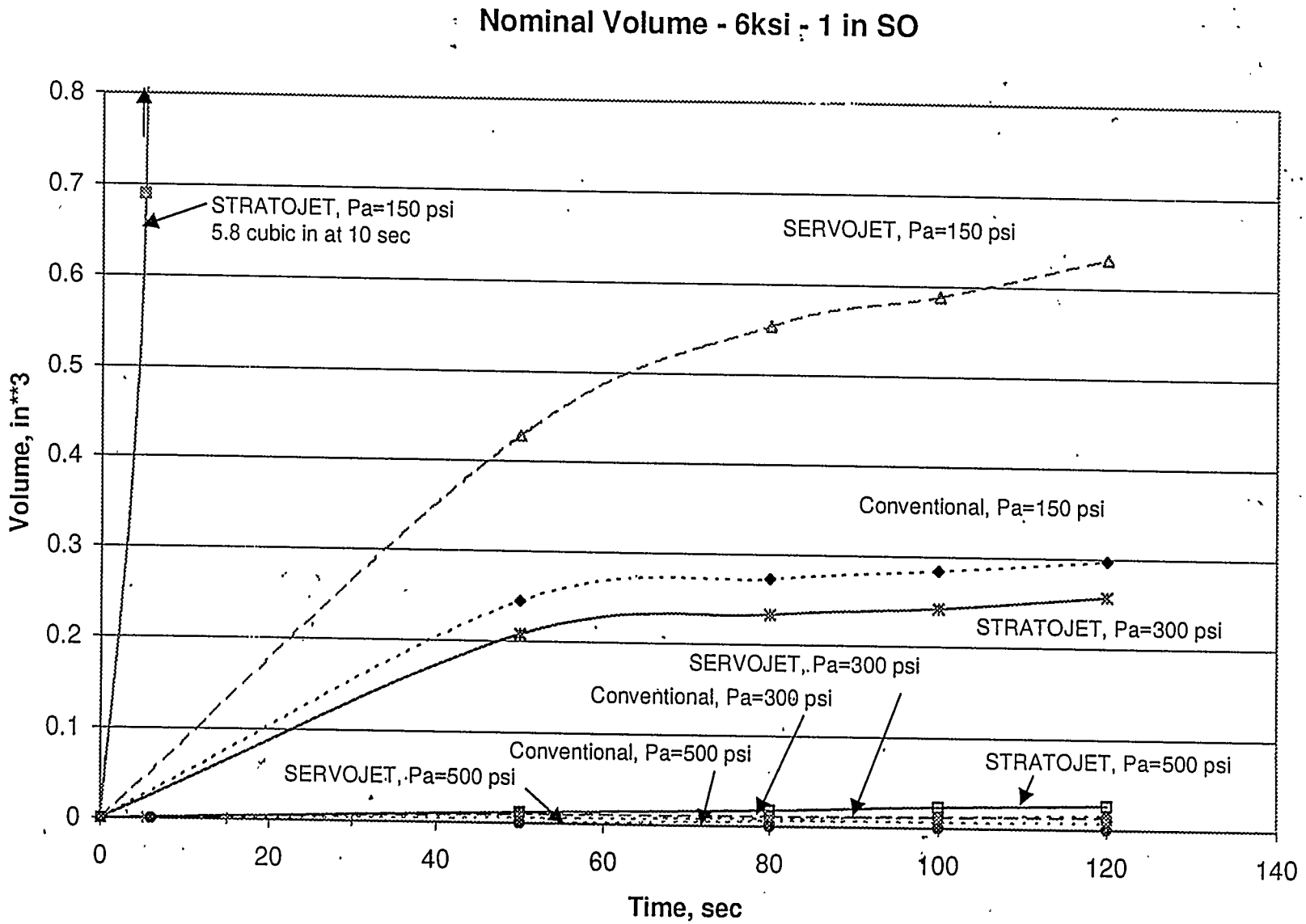

Figure 13. Progression of Volume of Erosion with Time for Three Nozzle Types and Three Ambient Pressures. Standoff = 1.0 in., ΔP = 6,000 psi, Flow Rate = 5.9 gpm.

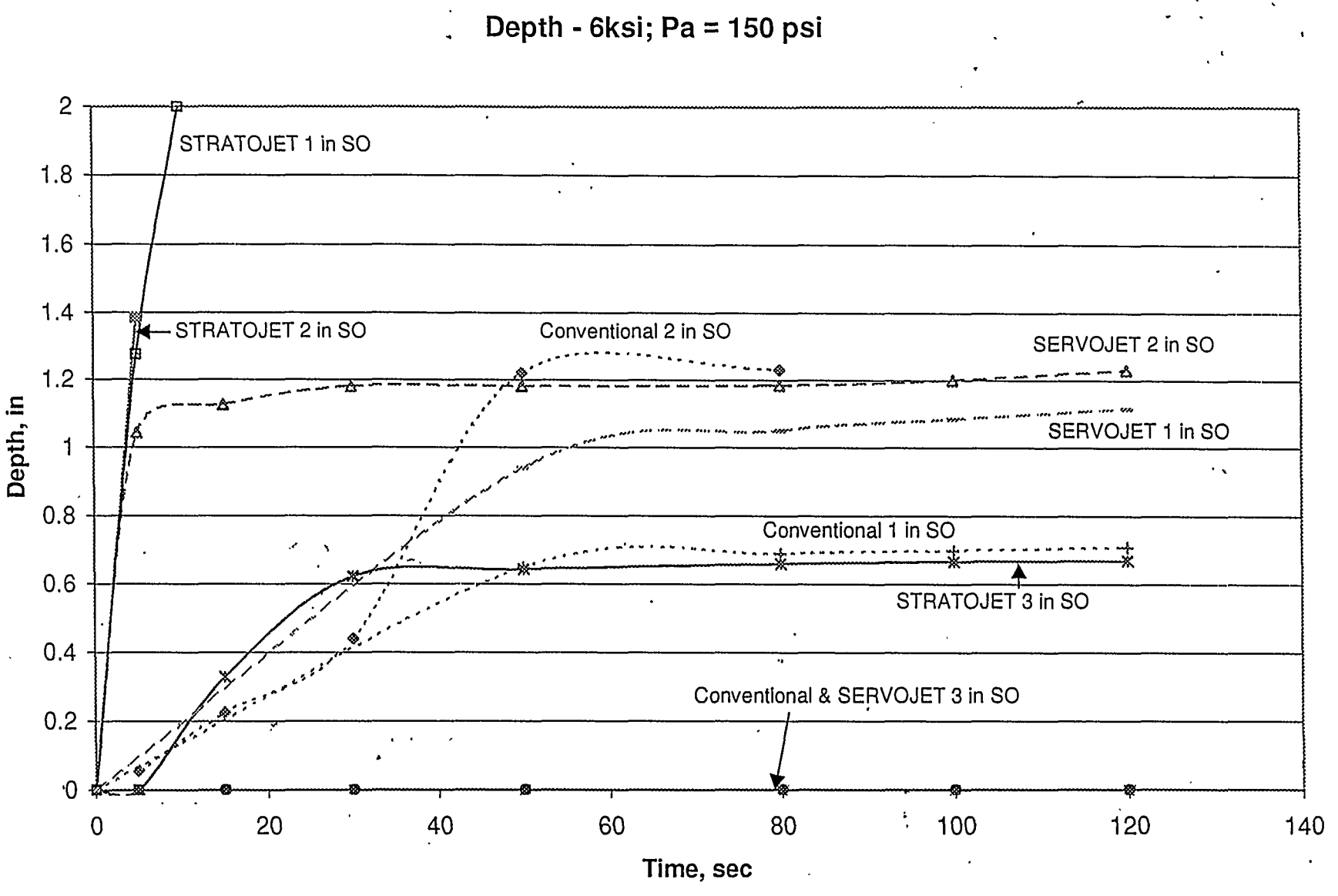

Figure 14. Influence of Standoff on Progression of Depth of Erosion with Time for Three Nozzle Types. ΔP = 6,000 psi, P_a = 150 psi, Flow Rate = 5.9 gpm.

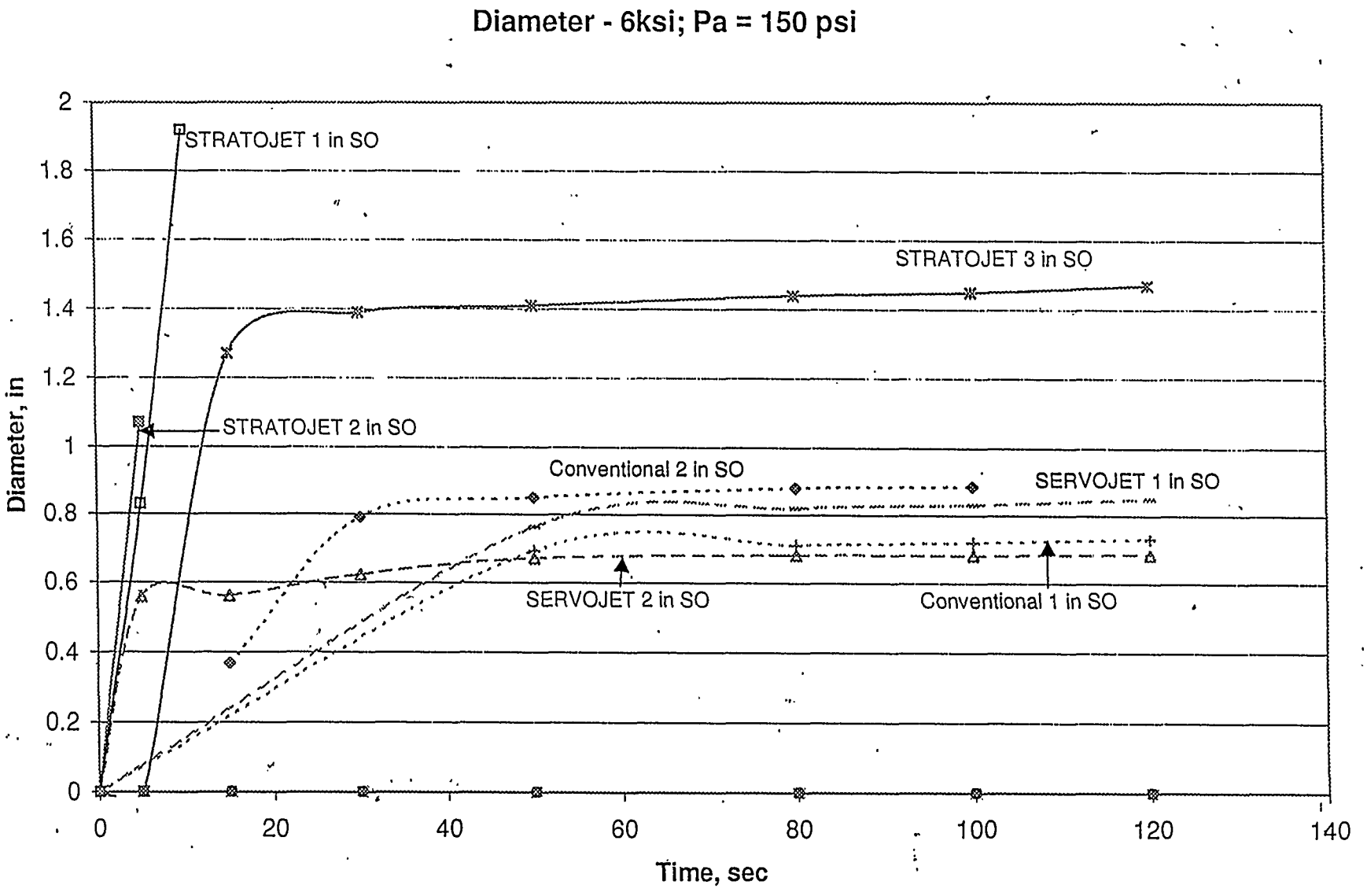

Figure 15. Influence of Standoff on Progression of Diameter of Erosion with Time for Three Nozzle Types. ΔP = 6,000 psi, P_a = 150 psi, Flow Rate = 5.9 gpm.

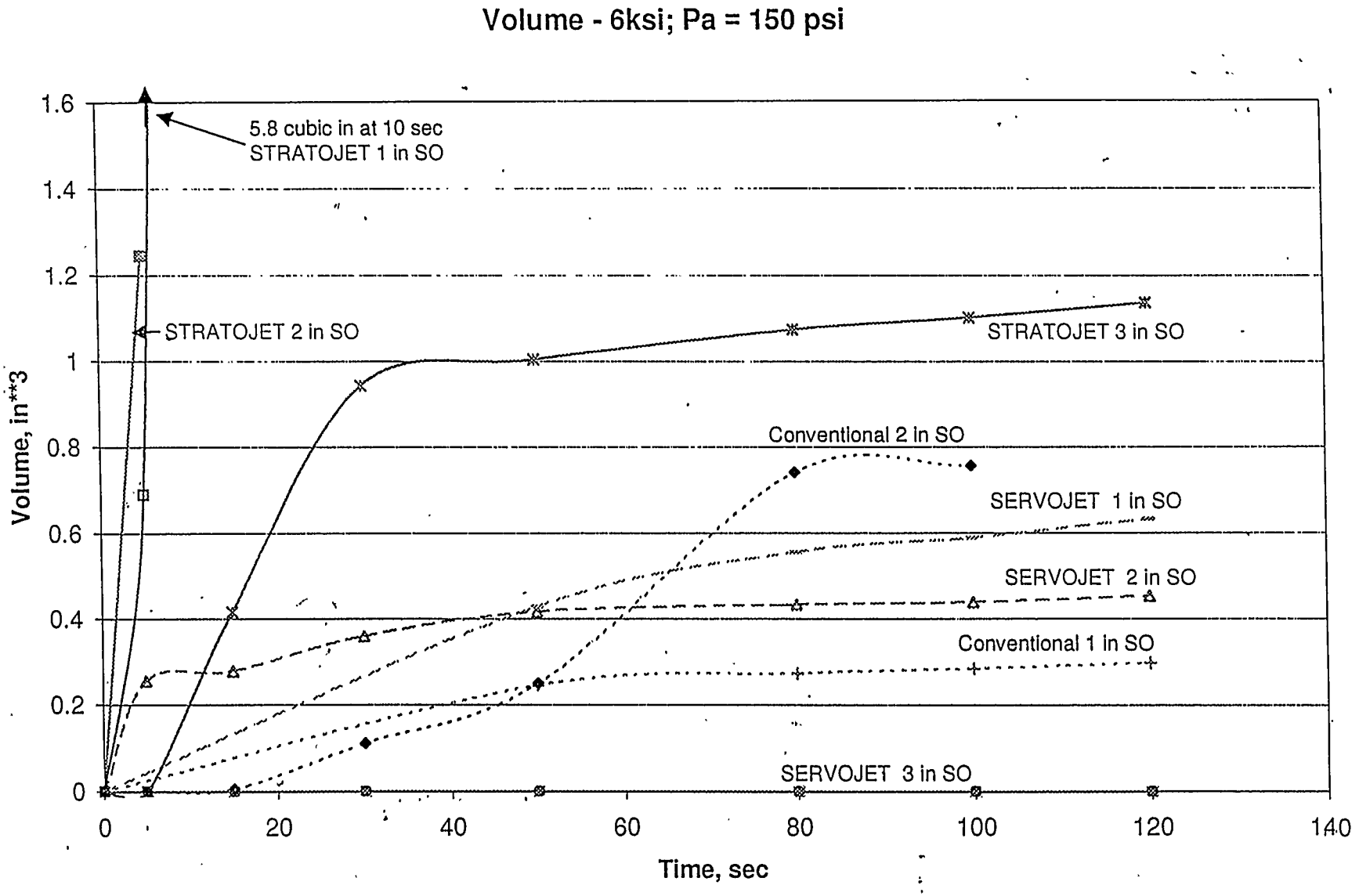

Figure 16. Influence of Standoff on Progression of Volume of Erosion with Time for Three Nozzle Types. ΔP = 6,000 psi, P_a = 150 psi, Flow Rate = 5.9 gpm.

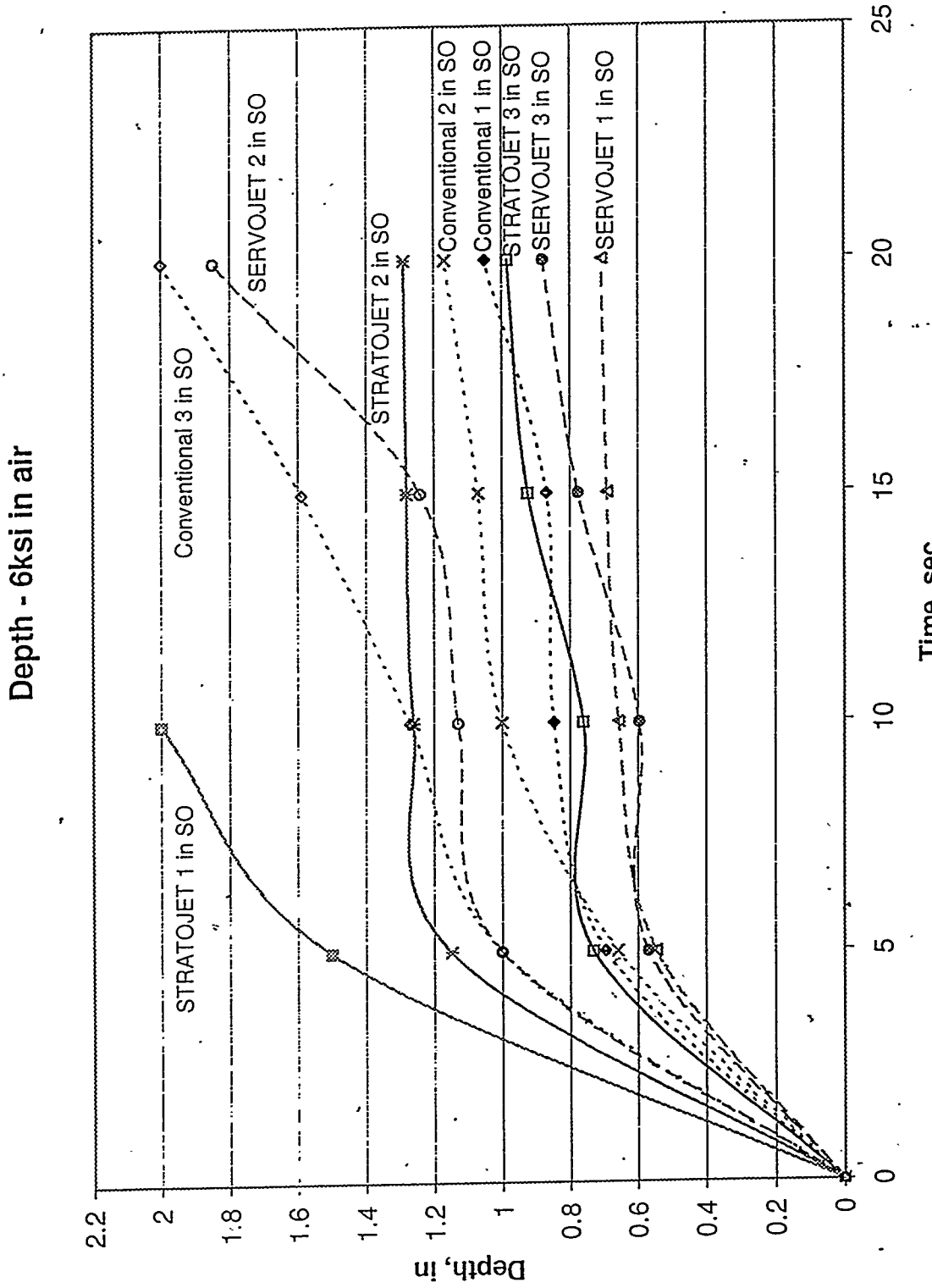

Figure 17, Influence of Standoff on Progression of Depth of Erosion with Time for In-Air Operation of Three Nozzle Types. $\Delta P = 6{,}000$ psi.

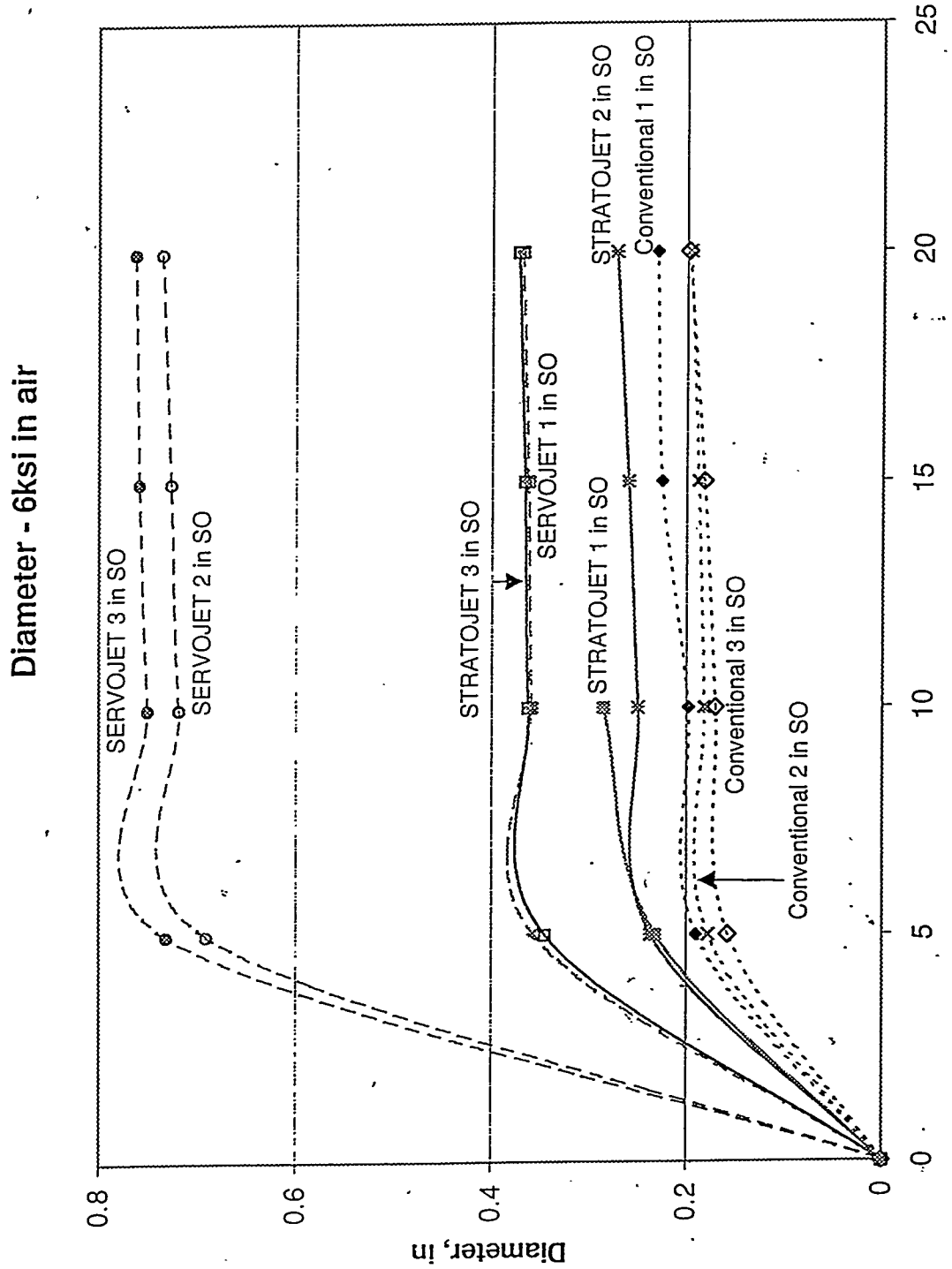

Figure 18. Influence of Standoff on Progression of Diameter of Erosion with Time for In-Air Operation of Three Nozzle Types. $\Delta P = 6{,}000$ psi.

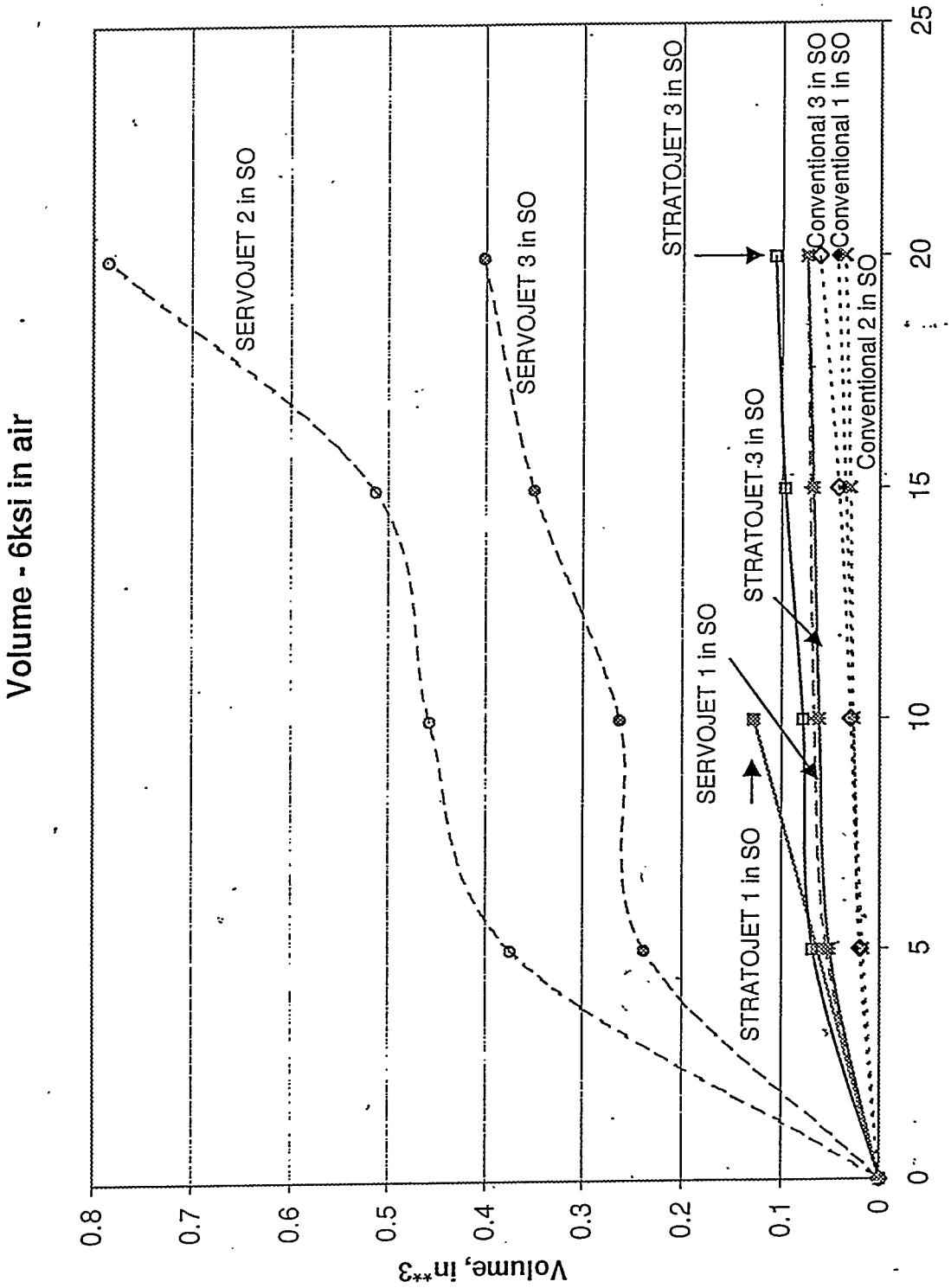

Figure 19. Influence of Standoff on Progression of Volume of Erosion with Time for In-Air Operation of Three Nozzle Types. ΔP = 6,000 psi.

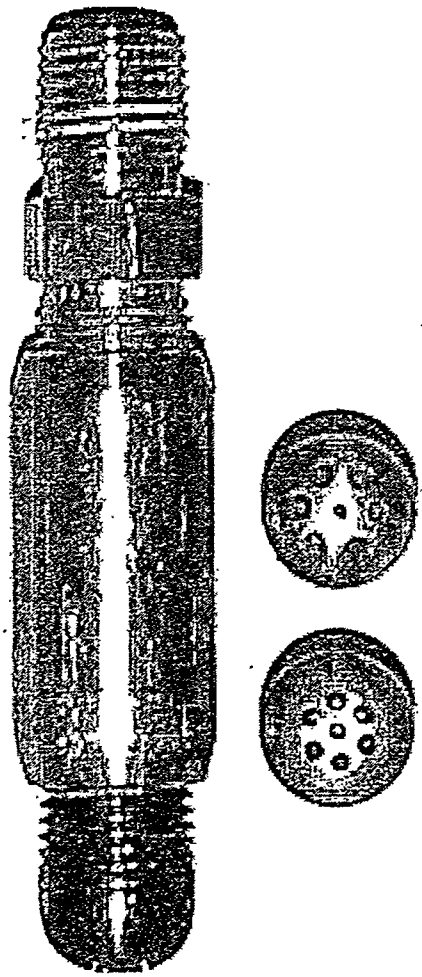

Figure 20. Photograph of Multi-Orifice STRATOJET® Nozzles and the Coupling Assembly Used to Advance the Nozzle. Each Nozzle Has a Central Orifice Surrounded by a Ring of Six Equally Spaced Orifices.

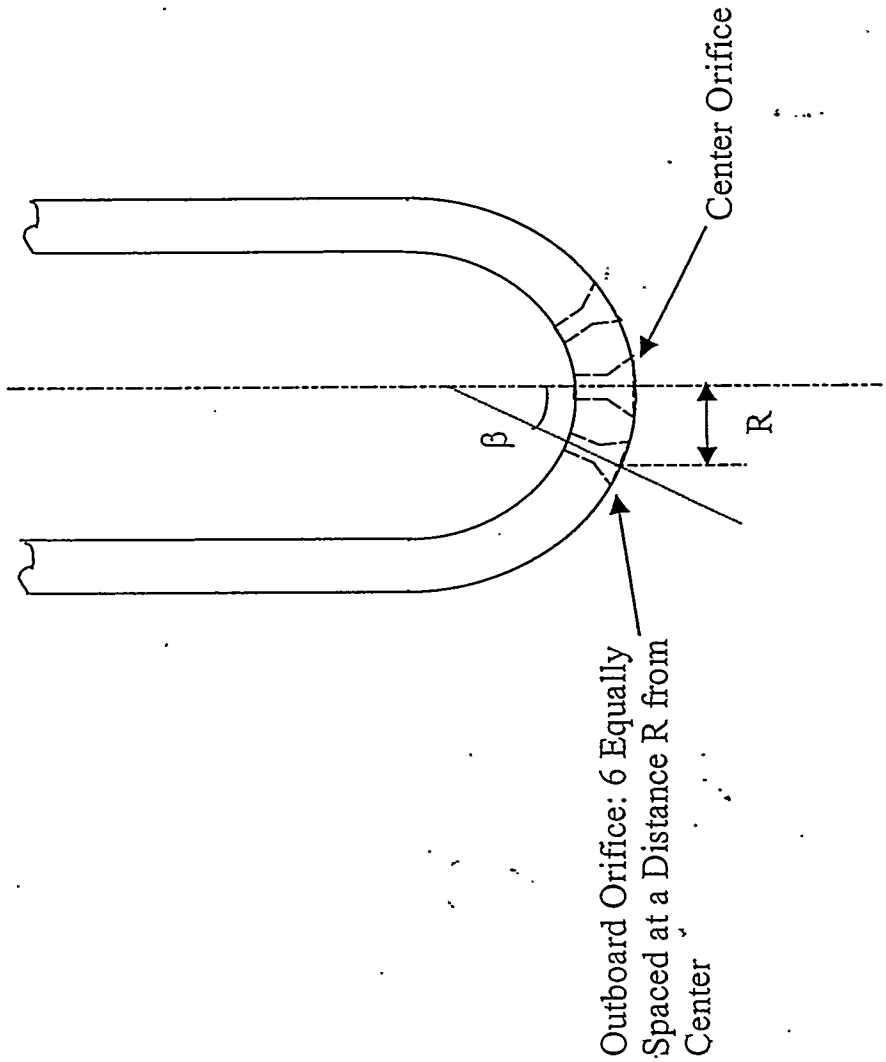

Figure 21. Sketch of Multi-Orifice STRATOJET® Nozzle Designs for Nozzles Show in Figure 20.

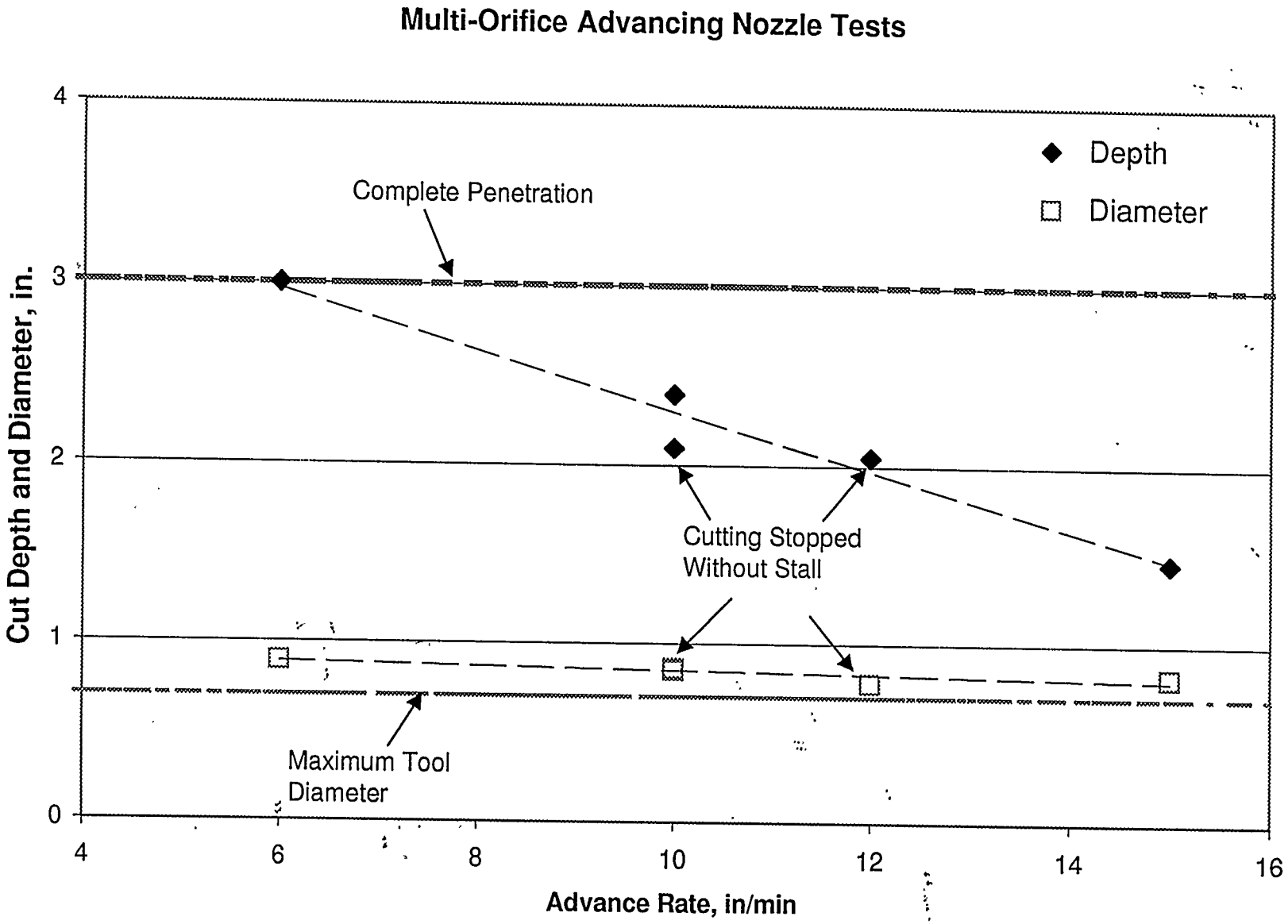

Figure 22. Results of the 7-Orifice STRATOJET® Nozzle Configuration II-B (Table 1) Advancing in Limestone at Different Rates. ΔP = 6,000 psi, P_a = 300 psi. A Cut Depth of 3 in Corresponds to Complete Penetration of the Sample. The Coupling Size Producing the Maximum Tool Diameter (0.70 in) is Also Shown.